JJMIE

Volume 16, Number 3, June. 2022
ISSN 1995-6665
Pages 381 – 393

Jordan Journal of Mechanical and Industrial Engineering

Adaptive Neuro Fuzzy Inference System to Predict the Mechanical Properties of Friction Stir Welded AA7075-T651 Joints

Vaibhav S. Gaikwad[1,*], Satish S. Chinchanikar[2]

[1]Research Scholar, Department of Mechanical Engineering, Vishwakarma Institute of Information Technology, Pune, Maharashtra State, India.
[2]Professor,Department of Mechanical Engineering, Vishwakarma Institute of Information Technology, Pune, Maharashtra State, India.

Received 17 Nov 2021 Accepted 10 Apr 2022

Abstract

The soft computing techniques are nowadays widely used in manufacturing industry for the modeling and optimization of processes parameters. The soft computing techniques give excellent predicted values which agree with the experimental results. In the present study, predictive model for the mechanical properties viz. ultimate tensile strength, micro hardness at weld nugget, and surface roughness in weld bead of friction stir weldedAA7075-T651 are developed. The adaptive fuzzy inference system technique is used for the development of the models. The models are developed using triangular, trapezoidal, Gaussian and generalized bell membership functions, and predicted values are compared. The triangular membership function shows minimum testing error of 19.1091, 12.3152, and 1.0018 for ultimate tensile strength, micro hardness at weld nugget, and surface roughness respectively. The validation experiment is performed at tool rotation speed of 1400 rpm and welding speed of 20 mm/min in order to check the predicted adaptive fuzzy inference system output. The observed values obtained after the validation experiment for ultimate tensile strength, micro hardness at weld nugget, and surface roughness are closer to the predicted adaptive fuzzy inference system output. The scanning electron microscopy images with energy dispersive X-ray spectrometer analysis confirmed the homogeneous mixing of material, laminar material flow with the equiaxed grain (size ~260 nm to 3 µm)distribution at the weld nugget. The scanning electron microscopy images of fractured tensile specimen shows the large dimple with the failure of specimen in heat affected zone.

Keywords: ANFIS, Membership functions, Mechanical Properties, FSW, AA7075.

1. Introduction

Friction stir welding (FSW) is a solid-state joining process. FSW is environment friendly, energy efficient, and versatile. Particularly, it can be used to join high-strength aerospace aluminum alloys and other metallic alloys that are difficult to weld by conventional fusion welding. FSW is considered to be the most significant development in metal joining in a last two decade [1].

FSW is an ideal solution for joining aluminum alloys; especially for the AA2000 and AA7000 series alloys. High-strength aluminum alloys, such as 7XXX, are commonly used in defense, aerospace, and military applications due to its high strength and light weight. These alloys are difficult to weld using conventional fusion welding as high temperature is involved in the processes, hence it can be joined through FSW. FSW has been successfully used in joining primary structures in the Eclipse 500TMjet [2].

VijayanandRao [3] developed a model to predict the tensile elongation and ultimate tensile strength (UTS) for friction stir welded (FSWed) AA2024 and AA6061 aluminum alloys. The models were developed using response surface methodology and adaptive fuzzy inference system (ANFIS). From this study, it was concluded that ANFIS predicted value has a greater accuracy and robustness in determining the values of dependent variables compared to the response surface methodology models. Eren et al. [4] performed a comprehensive review on the application of artificial intelligence (AI) techniques in FSW. Researchers attempted modeling of FSW using artificial neural network (ANN), machine learning, fuzzy logic, and meta-heuristic techniques and found prediction accuracy close to 95% with the experimental results. Attempts have been also made using ANFIS and machine learning techniques during FSW. Babu et al. [5] developed the model for prediction of mechanical properties of FSWedcryorolled AA2219 alloy using ANN. The genetic algorithm was used to determine the optimum FSW parameters. From

* Corresponding author e-mail: vsgaikwad113@gmail.com.

this study, it was found that ANN modeling can forecast the output responses with high accuracy and the least root mean square error (RMSE) value found from the batch back propagation was 0.0089991.

Teimouri and Baseri[6] developed the prediction model for UTS, % elongation and hardness of FSWed aluminum joints using fuzzy approaches. In this study two approaches were used; the first approach relationships between inputs and outputs based on human expertise were models using manually fuzzy models, then artificial bee colony algorithm (ABC) was used to modify these models. From this study, it was concluded that the combination of fuzzy-ABC system gives more accurate results as compared to manually fuzzy models. Zhao et al. [7] investigated the bobbin pin FSW of AA2219-T87. In this study the empirical models were developed for UTS and % elongation. The calculated R-squared (R^2) values for UTS and % elongation were 85 % and 75 % respectively. Choudhary et al. [8] implemented the hybrid particle swarm optimization (PSO) and genetic algorithm (GA) for optimization of submerged arc welding processes parameters. From this study, it was concluded that hybrid PSO-GA approach gives better solution than PSO and GA.

Safeen et al. [9] developed a mathematical model for prediction of mechanical properties which includes impact toughness, UTS, and hardness of the FSWedAA6061-T6 joints. In this study, response surface methodology along with central composite design was used. It was concluded from this study that welding speed of 70 mm/min, rotational speed of 1150 rpm, tool tilt angle of 3° with simple cylindrical pin profile, highest impact toughness, UTS, and hardness were all achieved.

Ahmadnia et al. [10] developed the model to predict the hardness, UTS, and elongation for FSWed AA6061 and AA5010 joints using response surface methodology. In this study, desirability approach was used for the optimization. The obtained optimization results shows that at tool rotational speed of 800 rpm, welding speed of 60 mm/min, and plunge depth of 0.25 mm/min are the optimal conditions which give 174 MPa UTS, 106 Hv hardness, and 33 % elongation. Choudhury et al. [11] used the integrated ANN and teaching learning based optimization (TLBO) soft computing modeling optimization to obtain the optimum processes parameters. In this study, UTS of the Inconel 825 super alloy joints produced using tungsten arc welding were optimized. ANN architecture with seven hidden layerneurons produce an effective error of 0.5% found optimum for predicting the UTS of the joints.

Hayajneh et al. [12] developed the prediction of surface roughness in end milling using two different gene expression programming. In genetic programming 1 and 2 model, the differences are their number of genes, head size, chromosomes, and the linking function. The R^2, RMSE and mean absolute percentage error are obtained as 0.923, 0.268 and 0.219 respectively, for all training set in genetic programming 1 model. Farouk et al. [13] perform the optimization of manufacturing tolerance using the goal programming method and the genetic algorithm. The table motion error, tool path error, and tool wear error were optimized using non-dominated sorting genetic algorithm (NSGA). The zero percent rejection was obtained by the optimization using goal programming and NSGA methodology. Soori et al. [14] performed the review of optimization procedures of machining parameters and applications of the different optimization methods, such as fuzzy logic algorithm, taguchi method, genetic algorithm, artificial intelligence, artificial neural networks and artificial bee colony algorithm, simulated annealing, ant colony optimization, PSO, scatter search technique, and response surface methodology and harmony search algorithm in optimization process of machining parameters.

Ismail [15] et al. used the machine learning techniques to detect fire fighting in power plant industry. One hidden layers and two hidden layers feed forward neural network models were developed for the prediction of occurrence of fire due to the impulsive burning of coal. From this study, it is proposed that two hidden layer feed forward neural network could be best fit for prediction of fire. Ning [16] schedule the resources in automobile part recycling using adaptive technique. Improved reverse PSO technique was used in this study. Using this methodology, the lesser energy consumption, highest recovery resource utilization rate, and the task time of about 200-400s were obtained. Ayun et al. [17] performed the optimization of injection moulding simulation parameters on performance measures viz. shrinkage and warpage of bone screw using PSO. The obtained results show that injection time, melt temperature, and packing time had significant effects on shrinkage and warpage of polylactic acid bone screws. The optimization results show that the shrinkage and warpage value improved to 2.4233% and 0.0928 mm for polylactic acid bone screws and 8.9592% and 0.4646 mm for polyglycolic acid bone screws.

Precup et al. [18] designed the model based fuzzy controllers for network control systems. In this study, Hilbert-Huang transform was applied for variable time delay to smooth the signals. Later on Takafi-Sugeno-Kang Proportional-Integral-Fuzzy design was applied for temperature controlled applications. From this study, it was concluded that the theoretical results were matched in excellent manner with the real-world temperature control applications. Vilela et al. [19] performed the value of information assessment for oil and gas industry by the application of fuzzy inference system (FIS). In this study, the use of a Boolean relationship between project valuation and project decision is replaced by the fuzzy inference system, a fuzzy human thinking approach to make decisions. To integrate more than one criterion into the assessment, the coherent method is used by the FIS as compared with the conventional value of information approach. In value of information approach, if more than criterion is used then the contradictory outcomes will be obtained which conduct to unconvincing assessment. Božanić et al. [20] implemented neuro-fuzzy system in decision making for the selection of construction machine (selection of loader). In this study, the data for neuro-fuzzy system is prepared using multi criteria decision making; logarithm methodology of additive weighs, VIekriterijumsko KOmpromisno Rangiranje, Technique for Order of Preference by Similarity to Ideal Solution. The developed model provides noteworthy support to decision makers for several reasons in selection of loader.

Meyghani et al. [21] performed the finite element modelling of FSW process on complex curved plate. In this study, software tools such as AltairHyperworks and ABAQUS software are employed for the simulation of the processes. The results obtained from the simulation show the significant increase in the heat generation, which results in the enlargement of the shear zone. Due to the enlargement of shear zone, the peak temperature rises to almost 300 °C after 3 seconds. Kavitha et al. [22] performed the optimization of FSW process for joining of AA7079 and AA8050 aluminum alloy using response surface methodology. The UTS of 211.48 MPa obtained at optimum values at tool rotational speed is 1000 rpm, welding speed of 300 mm/min, tool pin diameter of 2.4 mm, and shoulder diameter of 10 mm. Heidarzadeh et al. [23] developed the fuzzy model to predict the UTS and elongation of FSWed pure copper joints. In that study, 20 experiments were performed for the development of fuzzy model. Using fuzzy prediction model, the maximum UTS of 276.1 MPa and elongation of 44.6% was obtained at tool rotational speed of 1136 rpm, welding speed of 46.75 mm/min, and axial force of 3.34 kN.

Jamalian et al. [24] developed the ANN model for FSWed joints of AA5086-H34 plates which are reinforced with nanoparticles of Al_2O_3. The multi-pass technique by varying the tool pin was implemented in this study. The optimization results confirm that the highest UTS was obtained using square pin geometry which was of 303 MPa. Terra et al. [25] developed the models for FSW forces in case of square pin profile. In this study, the welding, tangential, transverse, and radial forces are demonstrated as a function of welding speeds, tool rotational speed and the instantaneous angle of rotation. The R^2values acquired are 0.9828, 0.9737, 0.9944, and 0.9881 for tangential, radial welding, and 0.9881 for the transverse force, which confirm the agreement between the models and experiments.

Han et al. [26] developed the ANFIS prediction model for hot deformation processes of Ti600 alloy. In this study, the ANFIS was integrated with back-propagation learning algorithm of neural network. The predicted values of ANFIS for the flow stress of Ti600 titanium alloy has a great accuracy and with absolute relative error less than 17.39%. Guneri et al. [27] implemented the ANFIS for the selection of supplier in the textile industry. The developed ANFIS model is robust with respect to the types of changes in the business. The ANFIS model is compared with the multiple regression model, and it is concluded that the ANFIS model performs better than multiple regression model. Naderloo et al. [28] developed the ANFIS model to predict the crop yield. The study includes higher number of input (eight inputs); two networks were trained. In ANFIS 1, the inputs were fertilizer, diesel fuel, and electricity energies, and in ANFIS 2 inputs were machinery, human labor, water for irrigation, chemicals, and seed energies. The RMSE and R^2 values were obtained as 0.013 and 0.996 for ANFIS 1 and 0.018 and 0.992 for ANFIS 2, respectively. Ekici et al. [29] developed the ANFIS model for the prediction of consumption of energy by the building in cold region. It was concluded from the study that ANFIS was efficient in predicting energy consumption of different buildings with a good degree of accuracy reaching 96.5% and 83.9% for heating and cooling respectively.

From the literature reviewed, it has been observed that numerous studies reported on modelling of weld qualities of the FSW process. However, researchers mostly attempted the modelling of processes parameters to predict the weld qualities using statistical techniques [30]. However, very few studies are available on the modelling of the processes parameters of the FSWed AA7075-T651 joints using soft computing techniques in the open literature. AA7075-T651 being low-weight and high-strength has been widely used in aerospace, automotive, and naval applications. However, this alloy showed poor weld ability due to porosity in the fusion zone and poor solidification microstructure. Hence, modelling of the process parameters while FSW of AA7075-T651 is crucial for obtaining a joint with better mechanical properties.

With this view, in the objective of the present study, to model the FSW processes parameters using ANFIS, to predict the weld qualities of FSWed AA7075-T651. In this study ANFIS model is developed using different membership functions. This paper will help the fellow researchers to select the best membership function and give the model to determine the mechanical properties of FSWed AA7075-T651 joints. Experiments were performed using the conical threaded tool varying the welding speed and tool rotation. Microstructural analysis and fracture behavior of FSWed joint is discussed for a better understanding of the process physics.

2. Experiment details

In the present study, FSWedAA7075-T651 square butt joints are produced. Experiments were performed on a universal milling machine. Two plates to be welded were initially squared and made free from any burr. The experimental setup is as shown in figure 1(a). A specially designed tool that provides thermo mechanical action along the weld direction due to its rotation and translation was used to get the required joint. A conical threaded tool pin with a constant plunge depth of 5.6 mm as shown in figure 1 (b) is used in the present study. The process parameters were selected based on the literature reviewed and pilot experiments. Experiments were performed under dry conditions and at tool rotations of 1000, 1200, 1400, 1600, 1800 and 2000 rpm, and at welding speeds of 20, 28, and 40 mm/min. A total of eighteen experiments were performed.

In this work, the mechanical behavior of the FSWed of AA7075-T651 joints is investigated in terms of the UTS, microhardness at weld nugget (MWN), and surface roughness (SR) at the center of the weld bead considering the effect of process parameters. The tool material used was H13 type tool steel and its geometry is a conical threaded pin type. The chemical composition of the tool material and workpiece material is depicted in Table 1 and Table 2, respectively. The UTS of base material was obtained as 550 MPa, with peak elongation of 9.1%.

The UTS of FSWed joints was measured using a universal testing machine. The test was performed as per the ASTME8M standard to obtain the transverse UTS of joints. Plate dimensions with positions for extraction of test specimens and tensile test specimens are as shown in figure 2(a) and (b) respectively. The MWN, was measured by Vicker's microhardness tester as per the ISO6507 standard. The diamond indenter with 136° and with a load of 100 grams for a dwell time of 20 seconds was used. The SR at the weld bead was measured by the surface roughness tester at 25 mm from the start of a weld, at the middle of the weld, and 25 mm before the end of the weld. An average of the three values measured at the said locations was noted down. The FSWed joint analysis was performed using field emission scanning electron microscope (FESEM) (Make: FEI Nova Nano SEM 450). The samples of size 5 x 5 mm were cut in transverse direction to weld line by wire electric discharge machining, and then it is observed under FESEM at different magnifications. The elemental analysis of weld nugget (WN) is carried out using Energy-dispersive X-ray spectroscopy (EDS) (Make: BrukerXFlash 6I30 spectrometer) in conjunction with scanning electron microscopy (SEM) images.

3. AdaptiveNeuro-Fuzzy Inference Systems Methodology

ANFIS is a model that incorporates both the fuzzy logic qualitative and adaptive neural network approaches and overwhelms their corresponding drawbacks. It is a good estimator and predictor. ANFIS has capability of approximation equal to the neural network; hence, the outputs can be easily constructed with ANFIS [3].

The ANFIS model contains five layers, and each of this layer is connected by numerous nodes. Each input node is extended by the preceding layer. The developed ANFIS models for UTS, MWN, and SR are presented in Figs. 3 (a), (b), and (c) respectively. The models shows that the network includes m inputs (M1, …,Mm), each of these inputs consists of n membership functions. In the present model is constructed by a layer with R fuzzy rules as an output layer. The product of number of membership function (n) and number of inputs (m) gives the total number of layers (N), i.e., ($N=n\cdot m$). The number of nodes in the other layer is related to the number of fuzzy rules (R). The details of each layer is mentioned as follows[3].

(a)

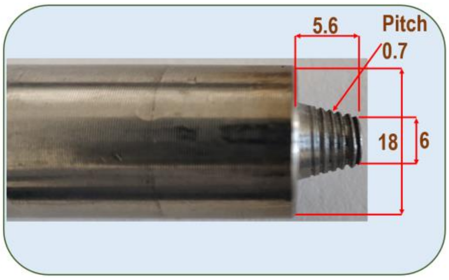

(b)

Figure 1. Friction stir welding a) Experimental setup, b) Conical threaded tool (all dimensions are in mm)

Table 1. The chemical composition (% weight) of H13 FSW tool [31]

Elements	Cr	Mo	Si	V	C	Ni	Cu	Mn	P	S
%	4.75	1.10	0.80	0.80	0.32	0.3	0.25	0.2	0.03	0.03

Table 2. Chemical composition (% weight) of AA7075-T651 alloy[31]

Elements	Si	Fe	Cu	Mn	Mg	Zn	Ni	Pb	Sn	Ti	Cr	Al
%	0.069	0.204	1.64	0.0060	2.33	5.28	0.012	0.012	<0.0050	0.028	0.195	90.22

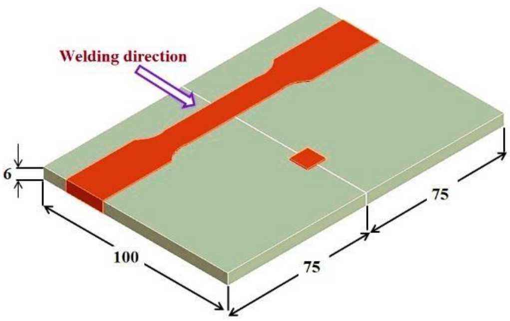

(a)

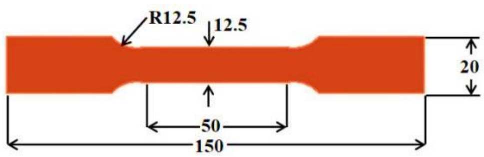

(b)

Figure2. a) Plate dimensions showing position for extraction of test specimens, b) Tensile test specimen (all the above-mentioned dimensions are in mm)

Layer 1 (fuzzification): The crisp inputs are transformed into the linguistic type using membership functions in layer 1. The output of this layer is expressed as,

$$Q_j^i = u_{ij}(X_i), \qquad i = 1 \dots m, \quad j = 1 \dots n \qquad [1]$$

Where u_{ij} is the j^{th} membership function for the input.

Layer 2 (product layer): In this layer, each fixed node can be obtained by multiplying the linguistic inputs, which were calculated in the previous layer:

$$Q_k^2 = W_k = u_{1e1}(X_1)u_{2e2}(X_2) \dots u_{me_m}(X_m),$$
$$k=1\dots,R;\ e_1, e_2, \dots, e_m = 1, \dots, n \qquad [2]$$

Layer 3 (normalized layer): For the each node the outputs were normalized using weighing factor as mentioned in equation [3].

$$Q_k^3 = \overline{W_k} = \frac{W_k}{W_1+W_2+W_3+\dots+W_R} \qquad [3]$$

Layer 4 (defuzzification layer): Takagi-Sugeno fuzzy-type if–then rules were applied in this layer to the output of each node.

$$Q_k^4 = \overline{W_k} f_k \qquad [4]$$

Where, f_k represents the output of k^{th} TSK-type fuzzy rules which is represented as follows:

If $(X_1\ is\ A_{1\,e_1})$ and $(X_2\ is\ A_{2\,e_2})$ and …….and $(X_m\ is\ A_{m\,e_m})$ then,

$$f_k \sum_{i=1}^{m} p_{ie_i X_i + r_k} \qquad [5]$$

Where, p_{ie_i, r_k} are called as consequent parameters and $e_1, e_2, \dots, e_m = 1, \dots, n;\ k = 1 \dots, R.$

Layer 5 (Output layer): The output modeled in the ANFIS is represented in this layer.

$$Q^5 = Y = \sum_{k=1}^{n} \overline{W_k} f_k \qquad [6]$$

To check the performance of the trained ANFIS model, RMSE is evaluated using the equation:

$$RMSE = \sqrt{\frac{1}{T}\sum_{z=1}^{T}(R_z - A_z)^2} \qquad [7]$$

Where, T is total number of training sample, R_z is the real output, and A_z is ANFIS output in training.

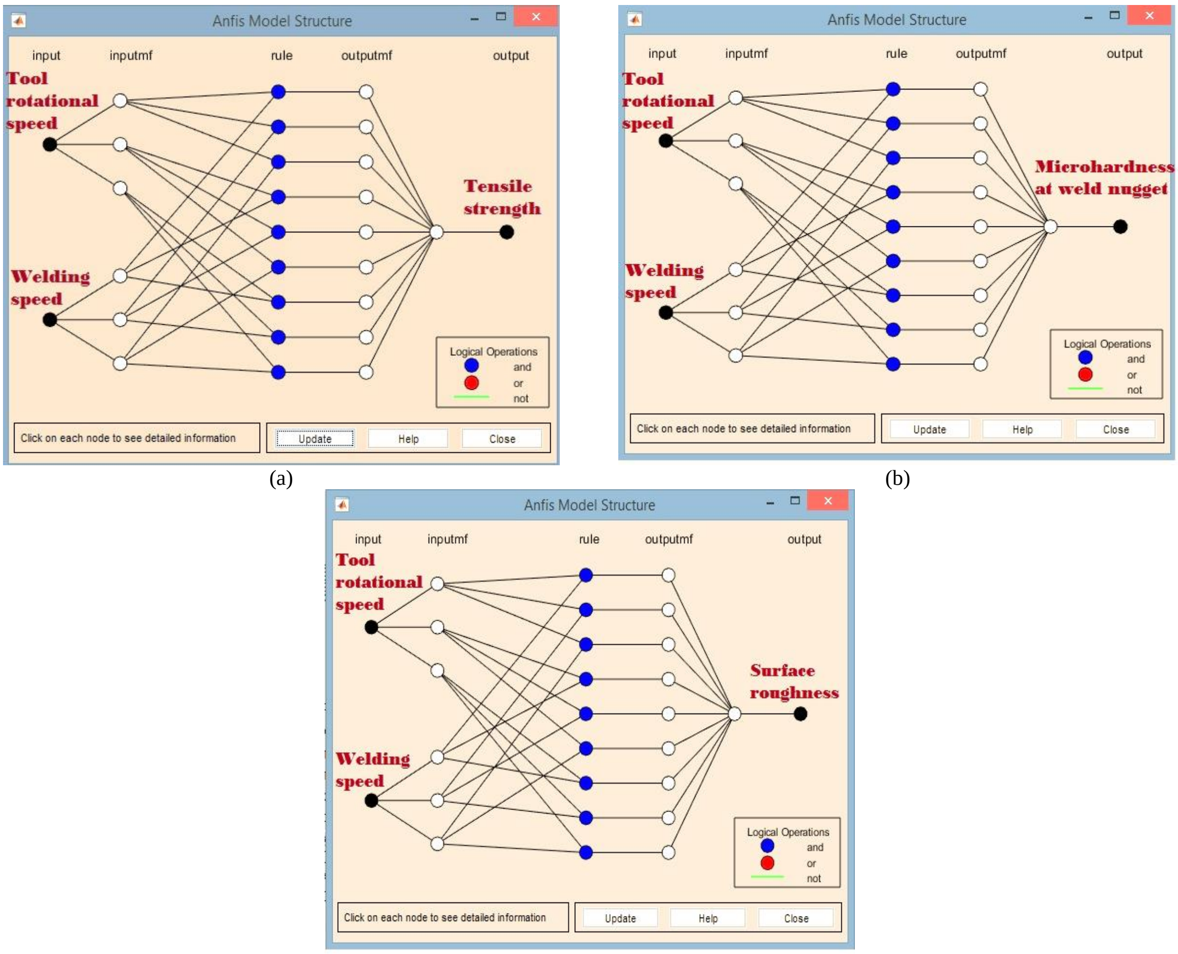

(c)

Figure 3. Developed ANFIS models structure for a) UTS b) MWN c) SR

4. Results and Discussion

4.1. Discussion based on ANFIS

The ANFIS model developed in the present study is using MATLAB R2022a. For predicting the mechanical properties viz. UTS, MWN, and SR of FSW process by ANFIS, the model consists of mainly two phases i.e. training phase and testing phase. The ANFIS model is established using thirteen dataset selected for the training. In the second stage, the trained network has been tested by other five additional data sets. Generally, the testing phase is executed in order to establish the pre-eminent network architecture of the network models.

In the present investigation three responses/outputs (UTS, MWN, and SR) are considered, hence three different models were trained. In ANFIS, the number of membership functions (MFs) and type of fuzzy rules, are considered to be the important factors to predict the accurate model. In the present study Sugenotype fuzzy-based rule has been used for the development of predictive models. The value for the error goal RMSE is set at 0.01 and the number of iterations is 300 epochs. This means, the training epochs are continued, until the RMSE fell below 0.01 or the epochs reach up to 300.

In the present study the number of MFs for input 1 (tool rotational speed) and input 2 (welding speed) are taken as three, and for the output UTS, MWN, and SR model is developed using the type of input MF as triangular (Trimf), trapezoidal (Trapmf), Gaussian (Gaussmf), and generalized bell (Gbellmf) MFs. The type of output MF is taken as a constant. Nine fuzzy rules are used in the present study. The triangular MF for input 1 (tool rotational speed) and input 2 (welding speed), and constant MF for output (UTS) are shown in figure 4 (a)-(c) respectively. Similarly input 1 (tool rotational speed) and input 2 (welding speed), and constant MF for outputs (UTS,MWN, and SR) can be shown using Trapmf, Gaussmf, and Gbellmf. The rules and rule viewer for the developed ANFIS model of UTS using Trimf is shown in figure 5 (a)–(b) respectively. Similarly the rules and rule viewer can be shown for the outputs UTS, MWN, and SR using Trapmf, Gaussmf, and Gbellmf.

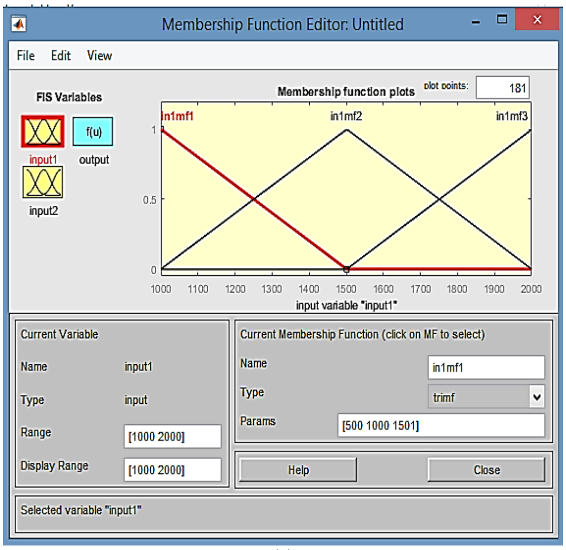

(a)

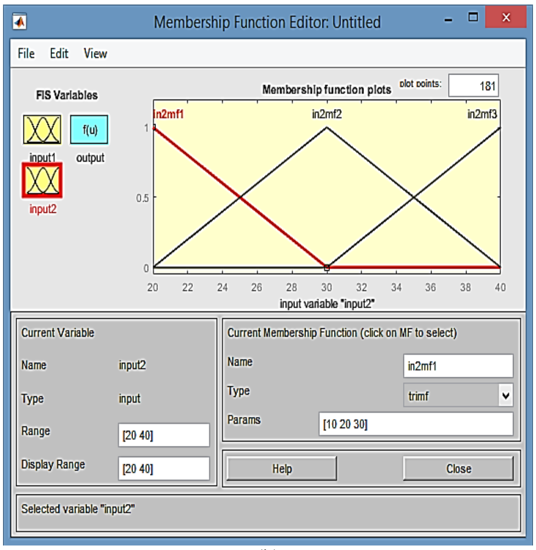

(b)

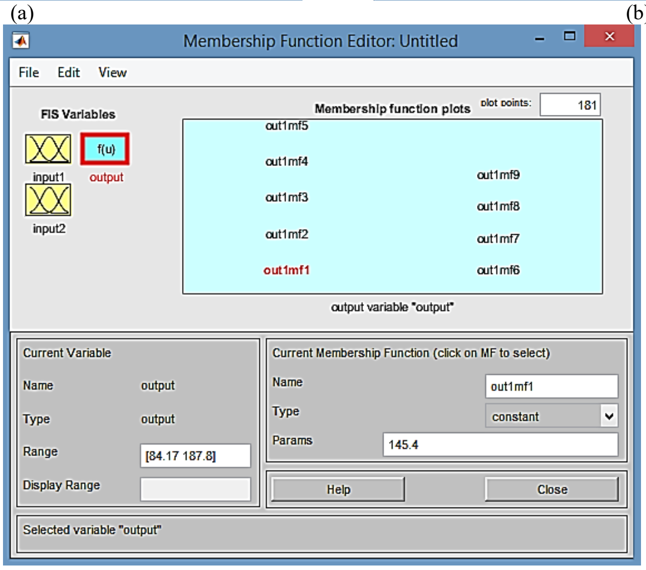

(c)

Figure. 5 a) triangular MF for input 1 (tool rotational speed) b) for input 2 (welding speed), and c) constant MF for output (UTS)

González et al. [32] developed the empirical model for FSWed Al 6061-T6-Cu C11000 joints. In this study, the correlation between performance measure corrosion resistance and input parameters of FSW such as the welding speed and tool rotational speed was established. The $R^2$for the developed model was obtained to be 0.85.Zhao et al. [33] developed the empirical model for the UTS and tensile elongation of FSWed AA2219-T87 aluminium alloy. The welding factors, such as shoulder pinching gap, tool rotational speed and welding speed are considered as inputs. The R^2 values for the UTS and tensile elongation was 0.85 and 0.75 respectively. Yuvaraj et al. [34] performed the optimization and empirical modelling of FSWed AA7075-T651 and AA6061 aluminium alloys. The tool offset, tilt angle, and pin profile were considered as the input parameters and UTS was considered as the output. The R^2value of the empirical model was around 0.98.

The predicted values of UTS, MWN, and SR are determined for each of these MFs. The R^2 values are determined in the present study for the UTS, MWN, and SR. The R^2 values of the output (UTS, MWN, and SR) obtained in the present study using Trimf, Trapmf, Gaussmf, and Gbellmf are greater than and in some cases closer to the R^2 values reported in the open literature [32-34]. Also the RMSE, testing error is determined and depicted in table 3.

It can be seen that the developed predictive models with triangular MF gives more accurate prediction of the mechanical properties. The minimum testing error of 19.1091, 12.3152, and 1.0018 is obtained for UTS, MWN, and SR using trimf respectively as compared with the trapmf, gaussmf, and gbellmf. Moreover, the better value of R^2 of 0.8639, 0.8178, and 0.9520 are obtained using trimffor UTS, MWN, and SR respectively as compared with the trapmf, gaussmf, and gbellmf.

The maximum testing error of 28.1289, 12.9314, and 1.3791 is obtained for UTS, MWN, and SR respectively using trapmf. Moreover the poor value of $R^2$are obtained as 0.7683, 0.7893, and 0.9321for UTS, MWN, and SR respectively using trapmf as compared with the trimf, gaussmf, and gbellmf.

It is noted that there is the marginal difference in the values of testing error and R^2 for gaussmf and gbellmf.

Experiment design matrix with their experimental, predicted ANFIS output using trimf, trapmf, gaussmf, and gbellmf for UTS, MWN, and SR are depicted in table 4.

The performance validation process of ANFIS based on UTS, MWN, and SR are presented graphically in figures7(a) −(c)respectively for trimf. The experimental values and ANFIS predicted values are scattered on both sides and are closer to the45° line, this indicates that the perfect fitness of the developed ANFIS models.

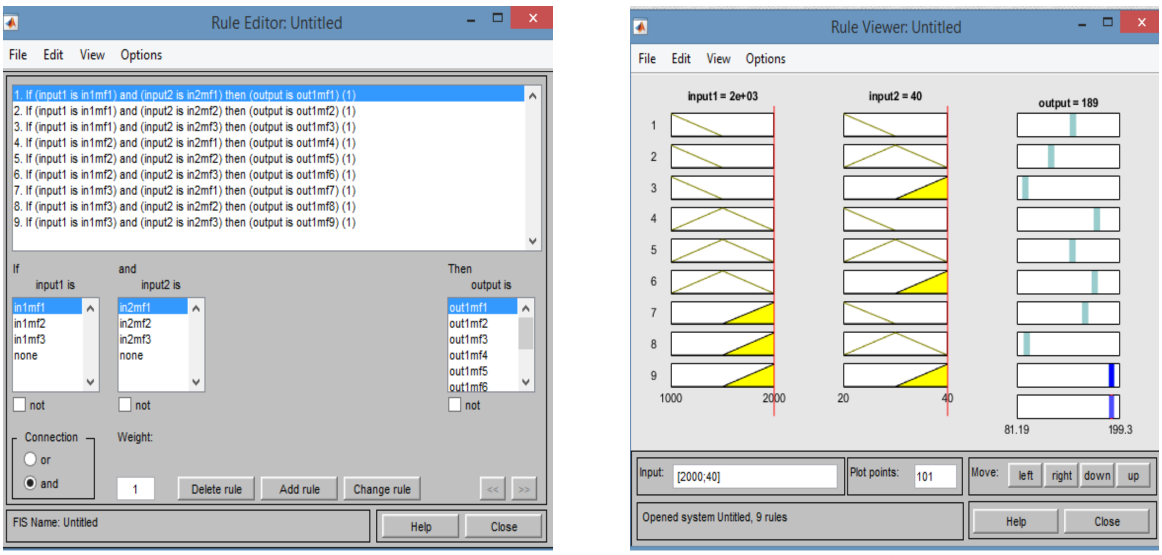

(a) (b)

Figure 6. a)Rules and b) Rule viewer for the developed ANFIS model of UTS using Trimf

Table 3. RMSE, testing error, and determination coefficient (R^2) for various MFs

Type of MFs	UTS			MWN			SR		
	Minimal training RMSE	Testing error	R^2	Minimal training RMSE	Testing error	R^2	Minimal training RMSE	Testing error	R^2
Trimf	12.9618	19.1091	0.8639	1.24801	12.3152	0.8178	0.494589	1.0018	0.9520
Trapmf	14.5044	28.1289	0.7683	0.902507	12.9314	0.7893	0.415752	1.3791	0.9321
Gaussmf	13.6566	22.0629	0.8302	0.968477	12.4863	0.8073	0.462078	1.1214	0.9477
Gbellmf	12.0391	22.3088	0.8525	0.777753	12.5225	0.7962	0.398903	1.2141	0.9482

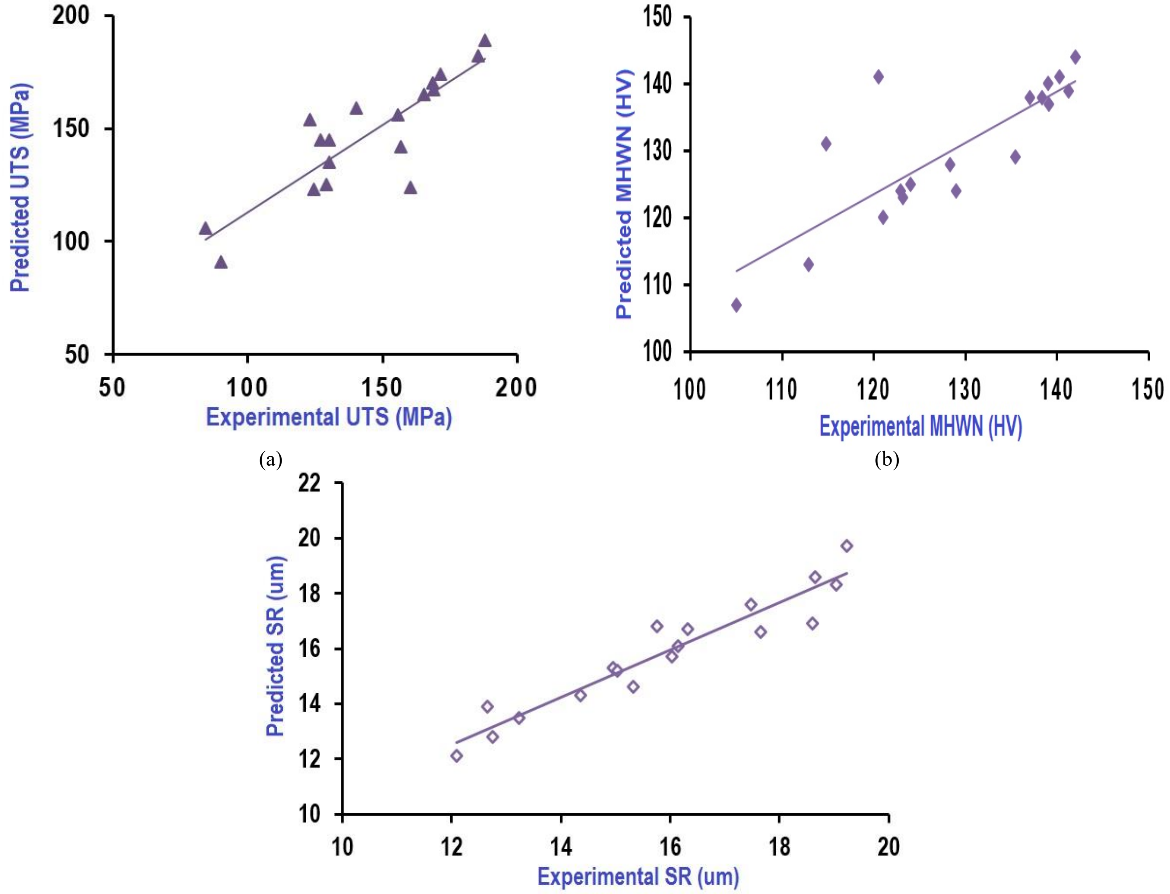

(c)

Figure7. Performance of predicted ANFIS output using trimf a)UTS, b)MHWN, and c) SR

Table 4.Experimental, predicted ANFIS output using trimf, trapmf, gaussmf, and gbellmf for UTS, MWN, and SR

Run	Tool rotation (rpm)	Tool transverse speed (mm/min)	Experimental values			Predicted UTS (MPa)				Predicted MWN (HV)				Predicted SR (μm)			
			UTS (MPa)	MWN (HV)	SR (μm)	Trimf	Trapmf	Gaussmf	Gbell mf	Tri mf	Trap mf	Gauss mf	Gbell mf	Tri mf	Trap mf	Gauss mf	Gbell mf
1	1000	20	130.020	105	12.65	145	151	148	149	107	110	109	110	13.9	14.4	14.2	14.4
2	1000	28	129.180	123.2	18.65	125	129	127	127	123	123	123	123	18.6	18.6	18.6	18.6
3	1000	40	90.070	138.4	12.1	91.1	96.2	93.3	92	138	138	138	138	12.1	12.2	12.1	12.2
4	1200	20	155.775	112.9304	14.9562	156	156	156	156	113	113	113	113	15.3	15	15.2	15
5	1200	28	130.225	128.956	17.485	135	131	133	133	124	123	124	123	17.6	18.1	17.8	18.1
6	1200	40	124.275	139.0504	12.7582	123	116	119	121	140	139	139	139	12.8	12.7	12.7	12.6
7	1400	20	168.830	121	17.65	167	169	168	168	120	122	120	121	16.6	16.7	16.6	16.9
8	1400	28	127.050	124	16.32	145	137	143	147	125	124	125	124	16.7	16.4	16.5	16.5
9	1400	40	123.110	120.5	13.23	154	174	160	164	141	141	141	141	13.5	14.3	13.7	14
10	1600	20	168.495	122.9704	15.7562	170	169	170	170	124	122	124	123	16.8	16.7	16.8	16.7
11	1600	28	156.705	135.476	18.605	142	137	140	147	129	124	128	125	16.9	16.4	16.7	16.8
12	1600	40	171.395	140.2904	14.3582	174	174	174	175	141	141	141	141	14.3	14.3	14.3	14.3
13	1800	20	165.255	128.3504	16.0362	165	165	165	165	128	128	128	128	15.7	16	15.8	15.9
14	1800	28	160.345	139.096	19.045	124	120	122	126	137	138	137	139	18.3	18.7	18.5	18.6
15	1800	40	185.355	141.2704	15.0382	182	185	183	181	139	139	139	139	15.2	15.5	15.3	15.4
16	2000	20	140.220	114.8	15.32	159	164	162	160	131	130	131	130	14.6	15.8	15.2	15.4
17	2000	28	84.170	142	19.23	106	114	110	100	144	143	143	142	19.7	19.5	19.6	19.5
18	2000	40	187.850	137	16.15	189	188	189	190	138	139	138	139	16.1	15.8	16	15.9

4.2. Discussion based on confirmatory experiment

In order to check the predictive values of ANFIS model, an additional confirmatory experiment is performed at tool rotation speed of 1400 rpm and welding speed of 20 mm/min. The UTS, microhardness at different zones of weld region, and SR is evaluated. The stress-strain curve, variation of microhardness in weld region, and top surface appearance of FSWed joint produced at 1400 rpm and 20 mm/min are shown in figures 8 (a)-(c) respectively.

The UTS, MWN, and SR obtained are 169.75 MPa, 122 HV, and 16.3 µm respectively at tool rotation speed of 1400 rpm and welding speed of 40 mm/min. It can be seen that the welded joint can sustain the load of 11.632 kN with % peak elongation of 4.9 %. The better tensile strength for FSWed joints can be obtained due to the better stirring of the material. The conical threaded pin increased the amount of material, both in transporting per revolution and extruding backward, resulting in more plastic deformation. It causes the fine grain size at the WN and higher UTS for FSWed joints.

The microhardness values of FSWed AA7075-T651 joints are measured at different points from the weld center on the advancing as well as the retreating side of the joint. The microhardness is measured in different zones of weld such WN, thermo mechanically affected zone (TMAZ), heat affected zone (HAZ), and base material (BM). Severe extrusion and higher plastic deformation during FSW causes variation in the grain size and the microhardness in the welded region. The microhardness of FSWed joints showed variation in the welding zone, mostly followed distribution a letter ‘W’ shape (fig.8 b) and found maximum at the WN and minimum at the heat affected zone(HAZ).

SR obtained on the weld top surfaces shows process effectiveness and generated surface is important from operational functioning of the welded joint. The figure 8 (c) shows the top surface appearance of confirmatory experiment. The proper mixing of material is observed at the weld line.

The heat generated in FSW results from the frictional effects of the rotating tool on the workpiece. The temperature is higher at highertool rotational speed and vice-a-versa. The temperature considerably increases across the weld samples as the rotating tool speed increases. This is due to greater frictional effects of the rotating tool on the workpiece as the rotational speedincreases leading to a higher amount of heat generation and consequently raising the weld temperature as reported by Abolusoro et al. [35].

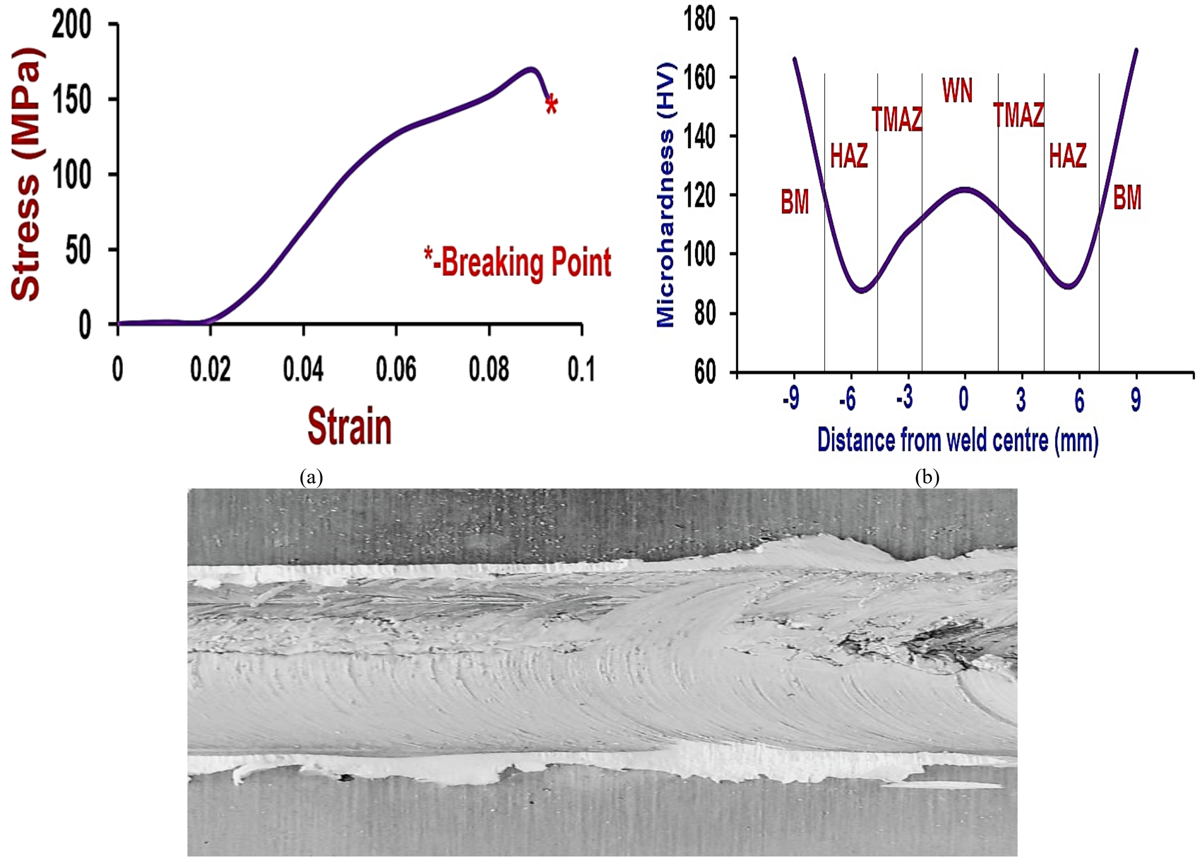

(c)

Figure8. a)Stress-strain curve b)Microhardness variation at different zones of weld, and c) Top surface appearance of weld

Figures 9 (a)-(c) represents the SEM images of WN, thermo-mechanically affected zone (TMAZ), and HAZ respectively for FSWed joint at tool rotation of 1400 rpm and welding speed of 40 mm/min. Figure 9 (a) depicts uniform grain distribution with ultra-fine grains having sizes in the range of 260 nm to 3 µm can be seen. A tunnel defect can be seen. The circular equiaxed grains are also observed in the WN. It can be seen that the grains in WN are fine as compared to TMAZ and HAZ. It could be attributed to higher heat generated in the WN due to more contact area of the conical threaded pin type tool. Due to higher heat generation in WN causes the dynamic recrystallization of grains resulting in finer grains.

Figure 9 (b) shows the SEM image of TMAZ. The pasty material flow,homogenous mixing of material is observed. The tunnel defect, and teared edge can be seen. The heat transferred from WN to TMAZ was adequate resulted in a homogeneous distribution of grain having a size in the range of 4-10 µm.

Figure 9 (c) depicts the SEM image of HAZ. Homogeneous distribution of grains with a uniform flow of material can be seen. However, the void, the elongated grain with the torn edge can be seen. The heat transferred from WN to HAZ is less (as compared TMAZ), hence teared edge with voids can be seen.

Beygi et al. [36] reported that contact area between tool and material plays an important role for obtaining quality weld. With the increase in the contact area between the tool and the workpiece, the axial load increases and fewer defects are formed due to the higher hydrostatic pressure. Further, the sticking condition increases the shearing contact area between the tool shoulder and material, and therefore, a greater quantity of material enters the shear plastic zone to be transferred around the tool. In the present study, the better results are using the conical threaded tool pin profile. The conical threaded tool pin profile provided more contact area that resulted in obtaining finer grain structure in WN, TMAZ, and HAZ.

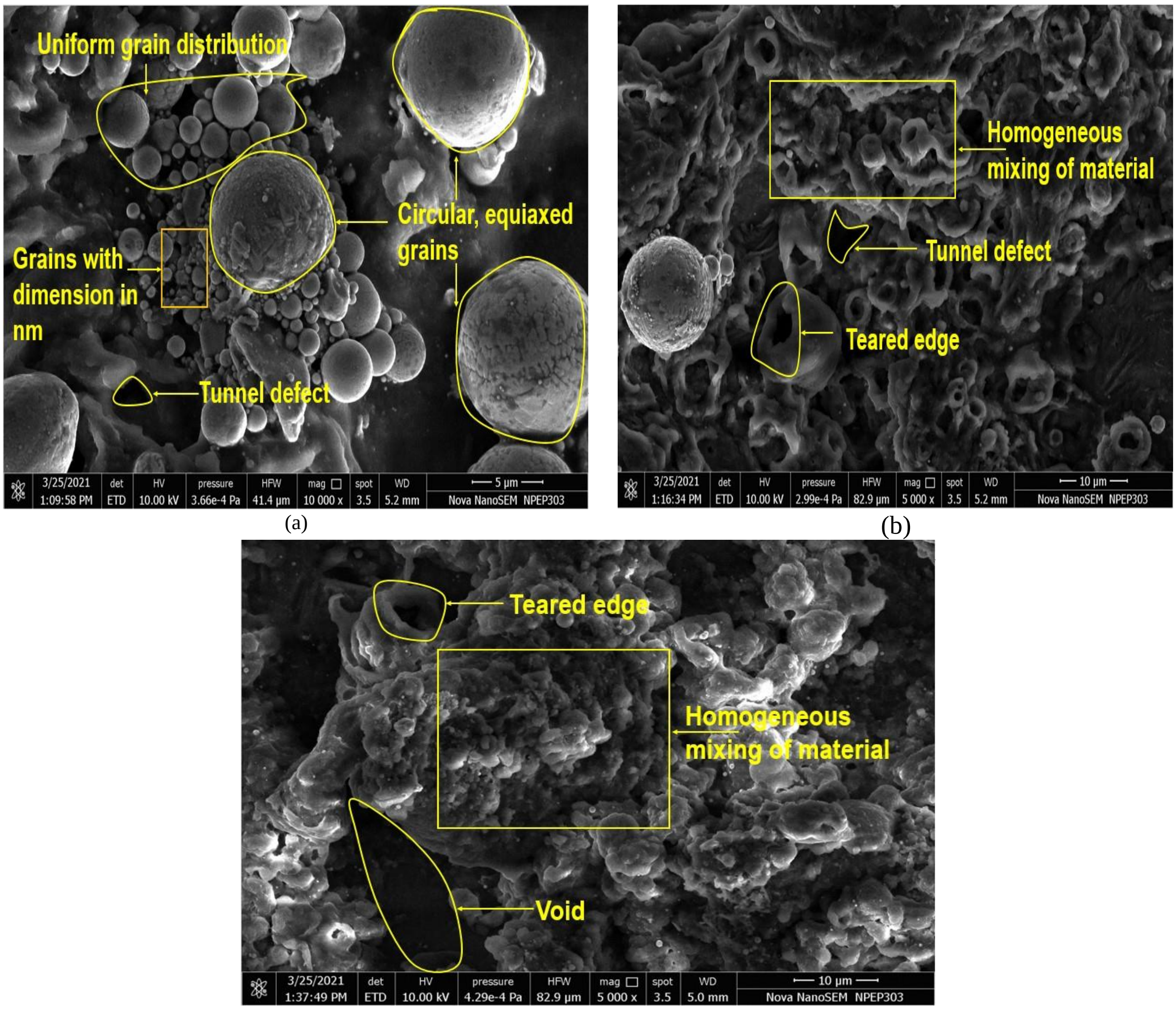

(a) (b) (c)

Figure 9.SEM images of a) WN, b) TMAZ, c) HAZ

Figures 10 (a) and (b) shows SEM image of the material flow in WN and fracture surface of tensile specimen of FSWed AA7075 joints. The weld quality can be determined considering the flow of pasty material beneath the FSW tool. From the fig. 10 (a), the laminar material flow with homogeneous mixing of material is seen. The larger contact area of conical threaded tool pin profile leads to the proper mixture material. The laminar material flow eliminates the defects and produce the joint with higher strength.

It can be seen from the fig.10 (b), that the large dimples are observed. The dimples shows the failure of specimen is ductile in nature. Moreover, the large size of dimples shows that the specimen can sustain a large amount of the load. It is seen that the fracture of specimen occurs in the HAZ. The HAZ shows coarser grain distribution, lower microhardness as compared to WN, TMAZ.

In the confirmatory experiment the EDS analysis is performed to check the presence of tool debris. The figure 11 (a) and (b) shows the SEM image captured and its EDS analysis respectively. The EDS analysis showed absence of any debris or any tool material element in the WN. The elements, such as Al, Cu, Mg, and Zn show majority of wt. % . The elements, such as Mn, Sn, and Ti disappear from the WN. The EDS microanalysis showed that the particles in the FSW joint mainly consist of the η(MgZn2) phase.

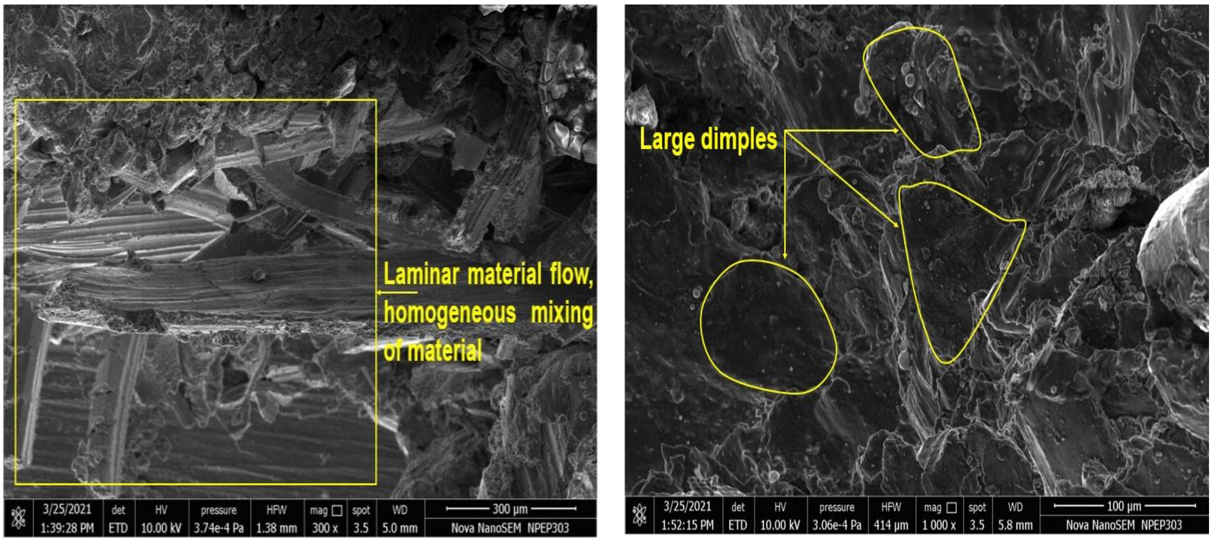

(a) (b)

Figure10.SEM image of a)Material flow in WN b)Fracture surface of tensile specimen

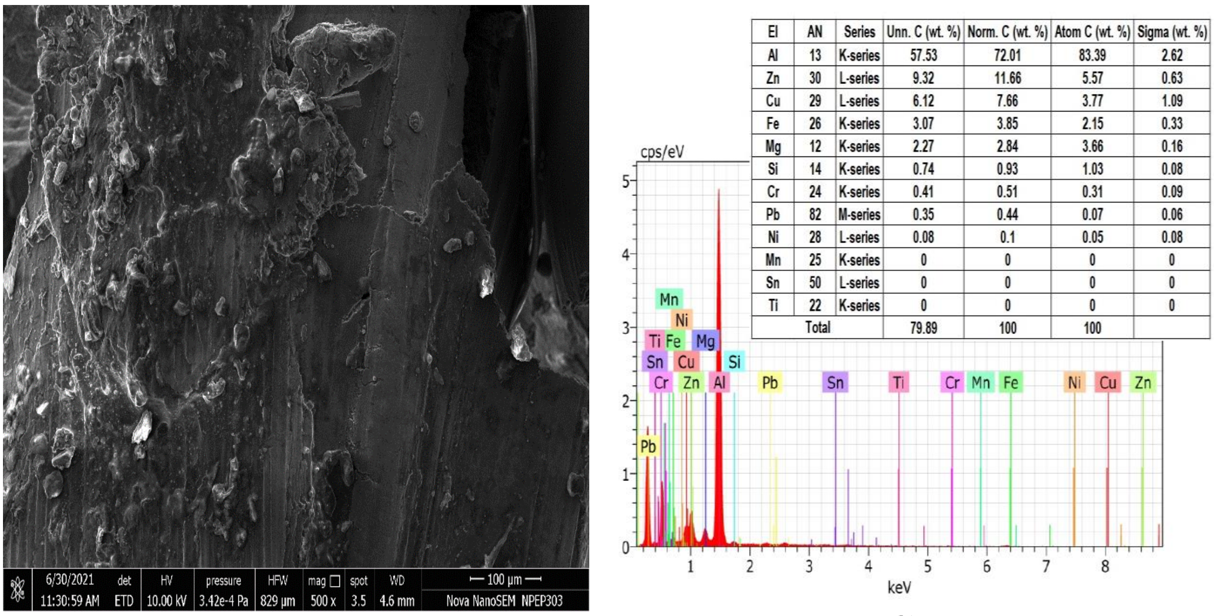

El	AN	Series	Unn. C (wt. %)	Norm. C (wt. %)	Atom C (wt. %)	Sigma (wt. %)
Al	13	K-series	57.53	72.01	83.39	2.62
Zn	30	L-series	9.32	11.66	5.57	0.63
Cu	29	L-series	6.12	7.66	3.77	1.09
Fe	26	K-series	3.07	3.85	2.15	0.33
Mg	12	K-series	2.27	2.84	3.66	0.16
Si	14	K-series	0.74	0.93	1.03	0.08
Cr	24	K-series	0.41	0.51	0.31	0.09
Pb	82	M-series	0.35	0.44	0.07	0.06
Ni	28	L-series	0.08	0.1	0.05	0.08
Mn	25	K-series	0	0	0	0
Sn	50	L-series	0	0	0	0
Ti	22	K-series	0	0	0	0
	Total		79.89	100	100	

(a) (b)

Figure11. a) SEM of at center of WN used for EDS b) EDS of WN

5. Conclusions

In the present study, the ANFIS model is developed for the mechanical properties viz. UTS, MHWN, and SR. The confirmatory experiment is conducted at tool rotational speed of 1400 rpm and welding speed of 20 mm/min. The microstructure at different regions in weld, material flow in WN, fracture behavior, and EDS analysis of FSWed AA7075 joint is investigated for the confirmatory experiment. The following conclusions could be drawn from the present work.

- The ANFIS model is developed to predict UTS, MHWN, and SR using trimf, trapmf, gaussmf, and gbellmf.
- The trimf shows minimum testing error of 19.1091, 12.3152, and 1.0018 for UTS, MHWN, and SR respectively as compared to trapmf,gaussmf, and gbellmf.
- The trapmf shows maximum testing error of 28.1289, 12.9314, and 1.3791 for UTS, MHWN, and SR respectively as compared to trimf, gaussmf, and gbellmf.
- The R^2 values obtained are 0.8639, 0.8178, and 0.9520 respectively for UTS, MHWN, and SR respectively using trimf.
- The SEM images shows the ultrafine grain in WN. The variation of grain size is observed as WN<TMAZ<HAZ<base material.

The overall presentation of the paper is a relatively short and simple in order to help to understand the flow of the paper. The model is not developed using other MFs.

Further study can be carried out to improve the current results using different prediction tools such as ANN. The study can be also extended to the optimization of process parameters using the developed ANFIS model.

References

[1] J. Zhang, P. Upadhyay, Y. Hovanski, and D. P. Field, "High-Speed Friction Stir Welding of AA7075-T6 Sheet: Microstructure, Mechanical Properties, Micro-texture, and Thermal History".Metallurgical and Materials Transactions A, Vol. 49, No. 1, 2018, 210–222.doi: 10.1007/s11661-017-4411-4.

[2] G. Elatharasan and V. S. S. Kumar, "Corrosion analysis of friction stir-welded aa 7075 aluminium alloy," strojniskivestnik - Journal of Mechanical Engineering, Vol. 60, No. 1, 2014, 29–34.doi: 10.5545/sv-jme.2012.711.

[3] D. Vijayan and V. Seshagiri Rao, "Parametric optimization of friction stir welding process of age hardenablealuminum alloys−ANFIS modeling," Journal of Central South University, Vol. 23, No. 8, 2016, 1847–1857.doi: 10.1007/s11771-016-3239-1.

[4] B. Eren, M. A. Guvenc, and S. Mistikoglu, "Artificial Intelligence Applications for Friction Stir Welding: A Review," Metals and Materials International, Vol. 27, No. 2, 2021, 193–219.doi: 10.1007/s12540-020-00854-y.

[5] K. Kamal Babu,K. Panneerselvam, P. Sathiya, A. NoorulHaq, S. Sundarrajan, P. Mastanaiah, C. V. Srinivasa Murthy, "Parameter optimization of friction stir welding of cryorolled AA2219 alloy using artificial neural network modeling with genetic algorithm," International Journal of Advanced Manufacturing Technology, Vol. 94, No. 9–12, 2018, 3117–3129.doi: 10.1007/s00170-017-0897-6.

[6] R. Teimouri and H. Baseri, "Forward and backward predictions of the friction stir welding parameters using fuzzy-artificial bee colony-imperialist competitive algorithm systems," Journal of Intelligent Manufacturing, Vol. 26, No. 2, 2015, 307–319.doi: 10.1007/s10845-013-0784-4.

[7] S. Zhao, Q. Bi, Y. Wang, and J. Shi, "Empirical modeling for the effects of welding factors on tensile properties of bobbin tool friction stir-welded 2219-T87 aluminum alloy," The International Journal of Advanced Manufacturing Technology , Vol. 90, No. 1–4, 2017, 1105–1118.doi: 10.1007/s00170-016-9450-2.

[8] A. Choudhary, M. Kumar, M. K. Gupta, D. K. Unune, and M. Mia, "Mathematical modeling and intelligent optimization of submerged arc welding process parameters using hybrid PSO-GA evolutionary algorithms," Neural Computing and Applications, Vol. 32, No. 10, 2020, 5761–5774.doi: 10.1007/s00521-019-04404-5.

[9] W. Safeen, S. Hussain, A. Wasim, M. Jahanzaib, H. Aziz, and H. Abdalla, "Predicting the tensile strength, impact toughness, and hardness of friction stir-welded AA6061-T6 using response surface methodology," The International Journal of Advanced Manufacturing Technology, Vol. 87, No. 5–8, 2016,1765–1781.doi: 10.1007/s00170-016-8565-9.

[10]M. Ahmadnia, S. Shahraki, and M. A. Kamarposhti, "Experimental studies on optimized mechanical properties while dissimilar joining AA6061 and AA5010 in a friction stir welding process," The International Journal of Advanced Manufacturing Technology, Vol. 87, No. 5–8, 2016, 2337–2352.doi: 10.1007/s00170-016-8636-y.

[11]B. Choudhury, M. Chandrasekaran, and D. Devarasiddappa, "Development of ANN modelling for estimation of weld strength and integrated optimization for GTAW of Inconel 825 sheets used in aero engine components," Journal of the Brazilian Society of Mechanical Sciences and Engineering, Vol. 42, No. 6, 2020.doi: 10.1007/s40430-020-02390-7.

[12] M. T. Hayajneh , M. Abdellahia, "Prediction performance of end-milling process by gene expression programming".Jordan Journal of Mechanical and Industrial Engineering, Vol. 13, No. 2, 2019, pp. 83–89.

[13] M. Farouk, R. Mohamed, S. Fethi, "Development of A New Technique for Modeling and Optimizing Manufacturing Errors for Cn Machine Tools". Jordan Journal of Mechanical and Industrial Engineering, Vol. 14, No. 4, 2020, pp. 381–386.

[14] M. Soori , M. Asmael, " A Review of the Recent Development in Machining Parameter Optimization". Jordan Journal of Mechanical and Industrial Engineering, Vol. 16, No. 2, 2022 pp. 205–223.

[15] F. B. Ismail, A. Al-Bazi, R. H. Al-Hadeethi, M. Victor, "A Machine Learning Approach for Fire-Fighting Detection in the Power Industry". Jordan Journal of Mechanical and Industrial Engineering, Vol. 15, No. 5, 2021, pp. 475–482.

[16] P. Ning, "An adaptive scheduling method for resources in used automobile parts recycling". Jordan Journal of Mechanical and Industrial Engineering, Vol. 14, No. 1, 2020, pp. 53–60.

[17] A.H.Q. Ayun, J. Triyono , E. Pujiyanto, "Optimization of Injection Molding Simulation of Bioabsorbable Bone Screw Using Taguchi Method and Particle Swarm Optimization".Jordan Journal of Mechanical and Industrial Engineering, Vol. 16, No. 2, 2022, pp. 319–325.

[18] R.E. Precup , S. Preitl , E. M. Petriu, C. A. B. Dragos, A. I. S. Stinean, R.C. Roman, E.L. Hedrea, "Model-based fuzzy control results for networked control systems" Reports in Mechanical Engineering, Vol. 1, No. 1, 2020, pp. 10–25, 2020.

[19] M. Vilela, G. Oluyemi, A. Petrovski, "A fuzzy inference system applied to value of information assessment for oil and

gas industry”. Decision Making: Applications in Management and Engineering, Vol. 2, No. 2, 2019, pp. 1–18.

[20] D. Božanić , D. Tešić , D. Marinkovic , A. Milić, “Modeling of neuro-fuzzy system as a support in decision-making processes”.Reports in Mechanical Engineering, Vol. 2, No. 1, 2021, pp. 222–234.

[21] B. Meyghani, M. Awang, C. S. Wu, “Finite element modeling of friction stir welding (FSW) on a complex curved plate”. Journal of Advanced Joining Processes, Vol. 1, No. January, 2020. doi: 10.1016/j.jajp.2020.100007.

[22] M. Kavitha , V. M. Manickavasagam, T. Sathish , B. Gugulothu , A. S. Kumar, S. Karthikeyan , R. Subbiah, “Parameters Optimization of Dissimilar Friction Stir Welding for AA7079 and AA8050 through RSM”. Advances in Materials Science and Engineering, Vol. 2021, 2021.

[23] A. Heidarzadeh, Ö. M. Testik, G. Güleryüz, R. V. Barenji, “Development of a fuzzy logic based model to elucidate the effect of FSW parameters on the ultimate tensile strength and elongation of pure copper joints”. Journal of Manufacturing Processes, Vol. 53, No. November 2019, 2020, pp. 250–259.

[24] H. M. Jamalian, M. T. Eskandar, A. Chamanara, R. Karimzadeh, R. Yousefian, “An artificial neural network model for multi-pass tool pin varying FSW of AA5086-H34 plates reinforced with Al2O3 nanoparticles and optimization for tool design insight”. CIRP Journal of Manufacturing Science and Technology, Vol. 35, No. 1, 2021, pp. 69–79.

[25] C. S. Terra, J. L. L. Silveira, “Models for FSW forces using a square pin profile tool”. Journal of Manufacturing Processes, Vol. 68, No. 1, 2021, pp. 1395–1404.

[26] Y. Han, W. Zeng, Y. Zhao, Y. Qi, Y. Sun, “An ANFIS model for the prediction of flow stress of Ti600 alloy during hot deformation process”. Computational Materials Science, Vol. 50, No. 7, 2011, pp. 2273–2279.

[27] A. F. Güneri, T. Ertay, A. Yücel, “An approach based on ANFIS input selection and modeling for supplier selection problem”. Expert Systems with Applications, Vol. 38, No. 12, 2011, pp. 14907–14917.

[28] L. Naderloo, R. Alimardani, M. Omid, F. Sarmadia,P.Javadikia, M. Y.Torabi, F. Alimardani, “Application of ANFIS to predict crop yield based on different energy inputs”. Measurement, Vol. 45, Vo. 6, 2012, pp. 1406–1413.

[29] B. B. Ekici, U. T. Aksoy, “Prediction of building energy needs in early stage of design by using ANFIS”. Expert Systems with Applications, Vol. 38, No. 5, 2011, pp. 5352–5358.

[30]S. Chinchanikar and V. S. Gaikwad, “State of the art in friction stir welding and ultrasonic vibration-assisted friction stir welding of similar/dissimilar aluminum alloys,” Journal of Computational and Applied Research in Mechanical Engineering, vol. 11, No. 1, 2021,67–100, 2021, doi: 10.22061/JCARME.2021.7390.1983.

[31]V. S. Gaikwad and S. Chinchanikar, “Mechanical behaviour of friction stir welded AA7075-T651 joints considering the effect of tool geometry and process parameters,” Advances in Materials and Processing Technologies, 2021, doi: 10.1080/2374068X.2021.1976554.

[32] F. A. Montes-González, N. A. Rodríguez-Rosales , J. C. Ortiz-Cuellar , C. R. Muñiz-Valdez, J. Gómez-Casas, J. S. Galindo-Valdés, O. Gómez-Casas, “Experimental analysis and mathematical model of fsw parameter effects on the corrosion rate of Al 6061-T6-Cu c11000 joints”. Crystals, Vol. 11, No. 3, 2021, pp. 1–19.

[33] S. Zhao, Q. Bi, Y. Wang, J. Shi, “Empirical modeling for the effects of welding factors on tensile properties of bobbin tool friction stir-welded 2219-T87 aluminum alloy”. International Journal of Advanced Manufacturing Technology, Vol. 90, No. 1–4, 2017, pp. 1105–1118.

[34] K. P. Yuvaraj, P. AshokaVarthanan, L. Haribabu, R. Madhubalan, K. P. Boopathiraja, “Optimization of FSW tool parameters for joining dissimilar AA7075-T651 and AA6061 aluminium alloys using Taguchi Technique,” Materials Today Proceedings, Vol. 45, 2021, pp. 919–925.

[35] O. P. Abolusoro, E. T. Akinlabi, S. V. Kailas,“Tool rotational speed impact on temperature variations, mechanical properties and microstructure of friction stir welding of dissimilar high-strength aluminium alloys”. Journal of the Brazilian Society of Mechanical Sciences and Engineering, Vol. 42, 2020, pp.176.

[36]R. Beygi, M. Kazeminezhad, M. Z. Mehrizi, G. Eisaabadi, A. Loureiro, “Friction stir butt welding of Al-Cu bilayer laminated composites: analysis of force, torque, and temperature”. International Journal of Manufacturing Technology, Vol.88, 2017, pp.393-400.